Biosensors and Bioelectronics 72 (2015) 362–369

Contents lists available at ScienceDirect

Biosensors and Bioelectronics

journal homepage: www.elsevier.com/locate/bios

# Quantum-dot biosensor for hybridization and detection of R3500Q mutation of apolipoprotein B-100 gene

Mohammad Mazloum-Ardakani [a,*], Roghayyeh Aghaei [a], Mohammad Mehdi Heidari [b]

[a] Department of Chemistry, Faculty of Science, Yazd University, Yazd 89195-741, Iran
[b] Department of Biology, Faculty of Science, Yazd University, Yazd 89195-741, Iran

ARTICLE INFO

*Article history:*
Received 21 March 2015
Received in revised form
5 May 2015
Accepted 6 May 2015
Available online 14 May 2015

*Keywords:*
CdS quantum dot
DNA biosensor
DNA hybridization
Apolipoprotein B-100 gene
Electrochemical impedance spectroscopy

ABSTRACT

A quantum-dot electrode system was developed as a transducer surface for covalent immobilization of a designed synthetic ApoB-100 specific probe, DNA hybridization and monitoring of DNA synthesis for the sensitive detection of R3500Q mutation of apolipoprotein B-100 (ApoB-100) gene. CdS-QDs cause an improvement in the fundamental characteristics of the electrode interface, such as its electroactive surface area, diffusion coefficient and electron transfer kinetics. The sensing characteristics of this biosensor offer a suitable potential for detection of target oligonucleotide with a detection limit of $3.4 \times 10^{-17}$ M. Also, the electrochemical responses of single-stranded DNA (ssDNA), DNA hybridization and DNA synthesis were investigated using electrochemical impedance spectroscopy (EIS). The extracted genomic DNA was detected based on changes in the charge transfer resistance (RCT) with $[Fe(CN)_6]^{3-/4-}$ as a redox probe. The proposed biosensor can distinguish between the normal sequence and the mutant sequence of ApoB-100 gene, promising a possibility to apply the QD-based biosensor for clinical investigations.



## 1. Introduction

Substantial progress over the past decade has led to dramatic improvements in the performance of biosensors. These improvements have, in turn, led to the fabrication of biosensors with capability of convenient measurement at less than subnanomolar (parts per trillion) levels (Wang and Liu, 2010, Benvidi et al., 2014; Thavanathan et al., 2014; Zhai et al., 2015; Amouzadeh-Tabrizi and Shamsipur, 2015; Huang et al., 2015). The best biosensor performance depends on biomolecular immobilization onto a suitable matrix. The interfacing of biomolecules with a nanomaterial may lead to producing a wide range of functional hybrid materials for biosensor applications. In comparison with bulk materials, nanoparticles can exhibit modified physical properties due to their size. For this reason, nanoparticles are very attractive in analytical detection systems and sensors (Lin et al., 2007; Gill et al., 2008; De et al., 2008). Nanostructured devices exhibit some improved properties such as enhanced catalytic activity or sensitivity (Katz et al., 2004; Mazloum-Ardakani et al., 2013, 2014a, 2014b, 2015; Taleat et al., 2014; Chen et al., 2007).

Quantum dots (QDs) are a novel class of inorganic nanoparticles which are gaining widespread recognition due to their exceptional photophysical properties (Wang et al., 2006). Colloidal quantum dot films allow large-area solution processing and bandgap tuning through the quantum size effect (Kramer and Sargent, 2011). Rapidly being applied to existing and emerging technologies, these films can play an important role in many fields (Algar et al., 2009; Klostranec and Chan, 2006; Zhang et al., 2010). QD-biocomposites, as a result of interaction of QDs with biological molecules including proteins, peptides and DNA, have widespread applications in areas ranging from in vivo imaging and diagnostics in biomedicine to environmental monitoring for public health and security (Prasuhn et al., 2010). A number of reports have shown that QD-conjugated oligonucleotide sequences (attached via surface carboxylic acid groups) may be targeted to bind with DNA or mRNA (Pathak et al., 2001; Gerion et al., 2002).

Electroanalytical chemists are attracted by QDs as a transducer surface for the development of electrochemical biosensing assays and keep in view various potentials of these nanoparticles (Sharma et al., 2013; Schubert et al., 2010). For instance, fabrication of a sensitive electrochemical biosensor using an interface based on QDs self-assembly for blood cancer detection has been reported by Sharma.

Effective coupling of quantum dots to biomolecules significantly depends on different synthesis methods of QDs and methods of surface modification with different ligands and capping agents (Murrar et al., 1993; Yu and Peng, 2002; Zhong et al., 2004). Therefore, solubilisation of QDs in water is essential for

* Corresponding author. Fax: +98 351 8210644.
*E-mail address:* mazloum@yazd.ac.ir (M. Mazloum-Ardakani).

http://dx.doi.org/10.1016/j.bios.2015.05.014
0956-5663/

many biological applications (Kim et al., 2004, Medintz et al., 2005, Chan et al., 2002).

Also, effective performance of QDs-based biosensors depends on the connection of QDs to the surface. Self-assembly is one of the most accepted methods for the fabrication of quantum dots films on conducting substrates (Asphahani et al., 2008).

The apolipoprotein B-100 (ApoB-100) mutation Arg 3500→Gln (R3500Q) causes reduced binding to the low-density lipoprotein (LDL) receptor and hypercholesterolemia (Soria et al., 1989). In most Caucasian populations studied so far, the underlying G→A substitution at nucleotide 10,708 in the ApoB gene occurs with a frequency about 1:500 (Tybjaerg-Hansen and Humphries, 1992), and one in about 50 individuals with hypercholesterolemia is a carrier (Myant, 1993). Thus, mutation is one of the most commonly inherited defects causing abnormality of lipid metabolism and increased risk of atherosclerosis. Genotyping of ApoB-R3500Q mutation has been done by PCR-RFLP and directed sequencing methods (Horvath et al., 2001). These techniques are relatively slow and very expensive in comparison to electrochemical techniques.

In this study, we demonstrate for the first time the use of a quantum-dots (QDs) electrochemical biosensor as a transducer surface for covalent immobilization of a designed synthetic ApoB-100 specific probe, DNA hybridization and monitoring of DNA synthesis. This is based on the immobilization of CdS-QDs on a gold electrode via formation of a self-assemble monolayer (SAM). The use of QDs on the electrode provides a larger surface area on the gold electrode compared to the bare electrode. Under optimal conditions, the biosensor can achieve high sensitivity to detect $3.4\times10^{-17}$ M of target DNA. Also, we investigated the synthesis of DNA following the attachment of the complementary target DNA. An increase in the DNA probe length after the denaturation process, which was confirmed by an increase in the $R_{CT}$ value of the biosensor, is demonstrative of DNA synthesis. An analysis performed with designed synthetic sequences and clinical patient samples indicate high potentials of this smart biosensor for initial screening of R3500Q Mutation of ApoB-100 Gene.

## 2. Materials and methods

### 2.1. Chemicals and oligonucleotides

Specific amine-terminated probes and primers were designed based on AGT gene obtained from the Gen Bank database. The oligonucleotides were designed by a primer design software (Premier 5.0, Premier Biosoft, Canada), and their secondary structure was examined with a Gene Runner (version 3.05, Hastings Software, USA). All the oligonucleotides were synthesized by Macrogen (Korea). Taq DNA polymerase and deoxyribonucleotide triphosphate (dNTP) were purchased from Sina Clon Company, Iran. The other chemical reagents used in the experiments included N-hydroxysuccinimide, N-(3-dimethylaminopropyl)-N'-ethylcarbodiimide hydrochloride, methylene blue, $CdCl_2\cdot2.5H_2O$ (99%), 3-mercaptopropionic acid (99%), thiourea (99%), and ethanol (HPLC grade). All the chemicals had analytical grades and were obtained from Sigma-Aldrich and Merck. All the solutions were prepared with deionized water. The solutions of probe and target oligonucleotides were prepared in a Tris–HCl buffer (20.0 mM Tris+20.0 mM NaCl) of pH 7.4 and stored at −20 °C. The designed synthetic oligonucleotide sequences, the other reagents and the instrumentation are introduced in the supporting information section (Section S1).

### 2.2. Self-assembly of CdS-QDs onto a gold electrode

To form a self-assembled monolayer (SAM) of CdS-QDs onto gold electrodes, freshly cleaned gold electrodes were incubated in a CdS-QDs solution containing N-ethyl-N′-(3-dimethylaminopropyl) carbodiimide (EDC; 0.2 M) and N-hydroxysuccinimide (NHS; 0.05 M) for four hours. The presence of EDC/NHS led to the activation of carboxylic groups on MPA-capped CdS-QDs. After incubation, the gold electrodes were rinsed with water to remove weakly attached CdS-QDs, followed by drying in air (experimental details for synthesis of CdS-QDs and preparation of Au electrodes are available in the Supporting information Sections S2, S3 and Scheme S1, Fig. S1).

### 2.3. Fabrication of pDNA/CdS-QDs/AU biosensor

The immobilization of amine-terminated probe DNA onto CdS-QDs/Au electrodes was performed for biosensor fabrication. The oligonucleotide monolayer was generated by treating the CdS-QDs/Au electrode with a 1 μM amine-terminated oligonucleotide solution (15 μL of pDNA was cast on the surface of the CdS-QDs/Au electrode) in a Tris−HCl buffer (0.1 M, pH 7.4) for five hours in a humid chamber at room temperature to allow amide bond formation with MPA-capped CdS QDs (Fischer, 2010). The fabrication of the pDNA/CdS-QDs/Au biosensor was followed by washing it with a Tris−HCl buffer (pH 7.4) to remove any unbound pDNA present on it surface and storing it at 4 °C after drying, where pDNA was a segment of the apoB-100 gene. To accomplish the hybridization, these biosensors were exposed to incubation with different concentrations of the target DNA (Scheme S2).

### 2.4. DNA hybridization assay and DNA synthesis

The quantum-dot oligonucleotide modified gold substrates were incubated for 30 minutes with the desired amount of target DNA in a hybridization buffer until double-stranded DNA (dsDNA) is formed. For DNA synthesis, 20 μL of a solution containing 2 μL of buffer, 2 μL of Klenow enzyme (5 U/μL), 2 μL of deoxyribonucleotide triphosphate (dNTP, 5 mM/μL), and 14 μL of water were casted on the surface of the dsDNA/CdS-QDs/Au biosensor. Then it was kept at 37 °C for an hour until strain complementary DNA was fabricated according to the model.

### 2.5. DNA amplification and gel electrophoresis of clinical samples

DNA was isolated from the peripheral blood samples using a DNA extraction kit (Gen fanavaran, Tehran, Iran). ApoB gene was amplified by PCR. PCR was performed in a total volume of 25 μL containing 100 ng of template DNA, 10 pmol of each primer, 200 μM dNTPs, 2.5 mM $MgCl_2$, 1 μL buffer, and 1 U of Taq polymerase. PCR amplification was carried out at 94 °C for five minutes, followed by 35 cycles of denaturation at 94 °C for 30 s, annealing at 60 °C for 30 s, and extension at 72 °C for 30 s, followed by a final extension for five minutes. The PCR products were electrophoresed on a 2% agarose gel and stained with ethidium bromide.

## 3. Results and discussion

### 3.1. Characterization of CdS@MPA QDs

In this approach, the synthesis of CdS-QDs involved mixing cadmium chloride, thiourea and 3-mercaptopropionic acid, followed by heating the reaction mixture in a sealed teflon tube at 100 °C. After an hour of growth, the original sharp excitonic

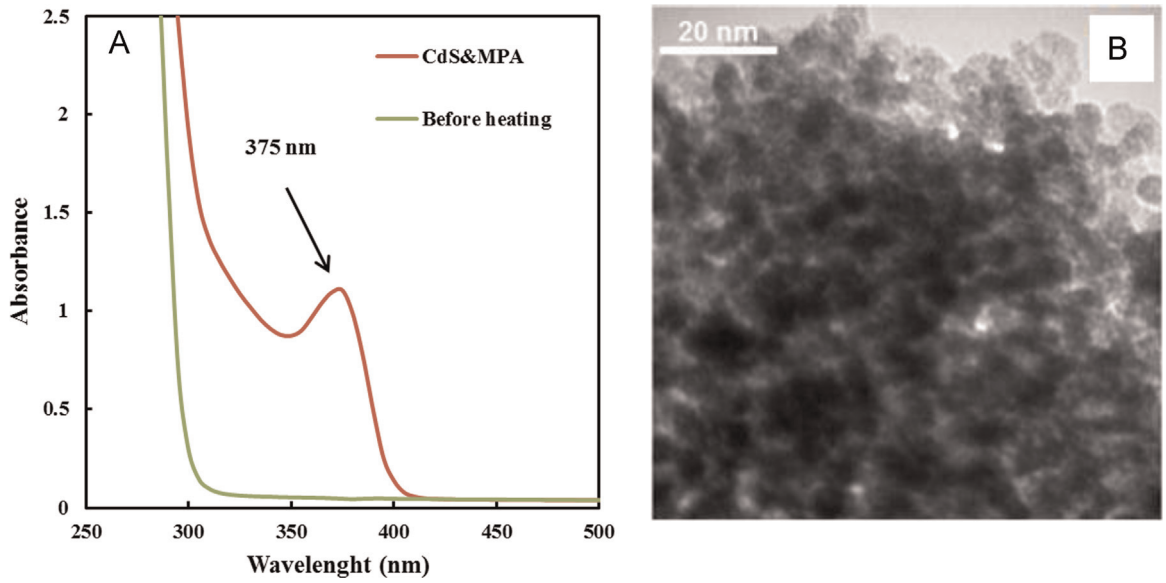


**Fig. 1.** (A) Absorption spectrum and (B) TEM image of CdS QDs.

absorption peak was observed at 375 nm, corresponding to the first excitation peak. This confirmed the formation of CdS@MPA (Fig. 1A) (Brus, 1984; Wang and Herron, 1991). The sharp absorption peak indicated that the particle size distribution was uniform. The sizes of the CdS-QDs were also estimated from the UV–vis absorption spectra by Peng's empirical equations (Yu et al., 2003) and were found to be in good accordance with the results obtained from the Brus formula. The results show that after a one-hour reaction, CdS-QDs was obtained with a diameter of 2.9 nm.

Fig. 1B shows a TEM image of the as-prepared CdS-QDs without any size selection after one-hour growth under the above-mentioned synthetic conditions. Monodisperse particles are observed with an average diameter of 3.0 nm.

### 3.2. Electrochemical properties of modified electrodes and biosensors

The electrochemical behavior of the electrodes and biosensors was studied in the potential range from −0.2 to 0.6 V at the scan rate of 30 mV/s, using cyclic voltammetric (CV) technique in a PBS (0.1 M, pH 7.4, 0.9% NaCl) solution containing 5 mM $[Fe(CN)_6]^{3-/4-}$. The cyclic voltammogram of the Au electrode in Fig. 2 (curve a) exhibits a sharp oxidation peak at 0.22 V with a peak current ($I_p$) value of 23.954 μA. After the self-assembly of the CdS-QDs onto the Au electrode, there was a sharp decrease in the $I_p$ value to 19.208 μA and a significant shift in the peak potential (0.28 V) as compared to the bare Au electrode (curve b, $\Delta E_p$= 0.15 V). This may be attributed to the semiconducting nature of CdS-QDs which leads to a slower electron transfer from the electrolyte to the electrode surface. After immobilization of 1 μM pDNA on the CdS-QDs/Au electrode, the $E_p$ value was further increased to 0.31 V (curve c, $\Delta E_p$= 0.21 V). Formation of an insulating layer on the electrode surface and the electrostatic repulsion between the negatively charged phosphate skeletons of the immobilized pDNA on the CdS-QDs/Au electrode and the anionic redox couple led to decreased electron transfer.

The control experiment was carried out by immobilizing pDNA onto the Au electrode using 3-mercaptopropionic acid as a cross-linker (pDNA/MPA/Au) (Li et al., 2009). A significant shift was observed in the peak potential (curve d, 0.36 V) compared to pDNA/CdS-QDs/Au. This can be attributed to a slower rate of electron transfer across the interface (Zoski, 2007).

There was a further increase of $\Delta E_p$ and decrease of the peak

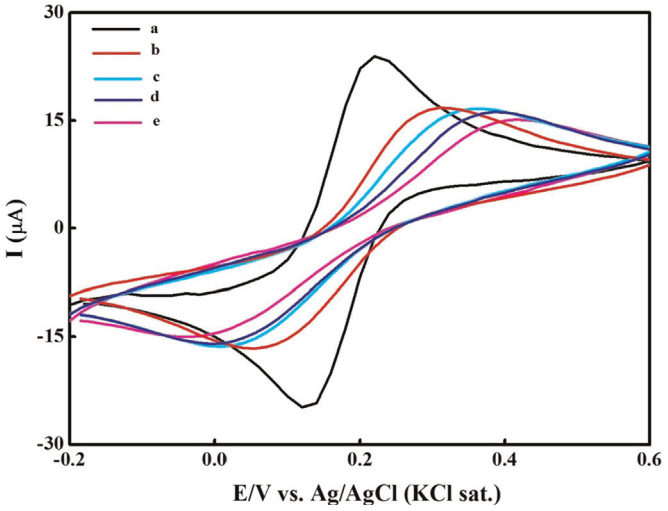


**Fig. 2.** Cyclic voltammograms in a PBS (0.1 M, pH 7.4, 0.9% NaCl) solution containing 5 mM $[Fe(CN)6]^{3-/4}$ for a Bare Au electrode (a), CdS-QDs/Au electrode (b), pDNA/CdS-QDs/Au biosensor (c), pDNA/MPA/Au (d) and after hybridization with $10^{-16}$ M concentration of its complementary DNA.

redox currents through hybridization of the DNA probe with the target complementary DNA ($10^{-16}$ M, curve e), which are ascribed to the more electrode surface blocking caused by hybridization and increasing repulsion between the negatively charged DNA hybrids and $[Fe(CN)_6]^{3-/4-}$ anions.

CV studies were carried out at various potential scan rates ($\upsilon$, 10–500 mV/s) to investigate the interfacial kinetics on the electrode and biosensor surface. As the scan rate was increased, the anodic and cathodic peaks of the electrodes and biosensors were found to move in opposite directions, suggesting that the redox process was quasi-reversible. The linear variation of the peak potential, as a logarithmic function of scan rate in the range from 10 to 500 mV/s, is depicted in Fig. 3A. Using Laviron's equations, the value of transfer coefficient ($\alpha$), for n number of electrons, was determined from the slope of two straight lines with anodic and cathodic slopes of $2.303RT/(1-\alpha)nF$ and $-2.303RT/\alpha nF$ respectively. The charge transfer rate constant ($k_s$) was calculated using Eq. (1) (Laviron, 1979).

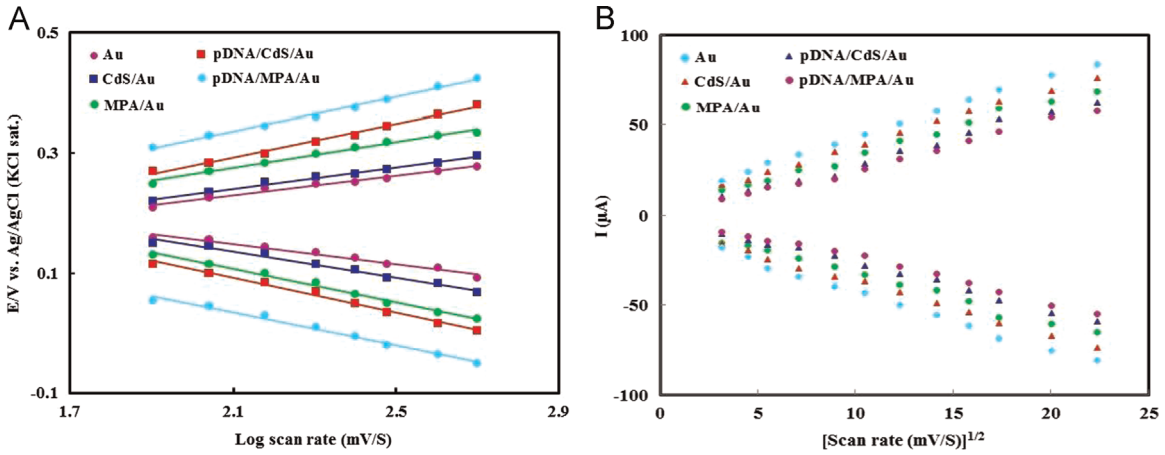


**Fig. 3.** Cyclic voltammogram variation of (A) potential vs. log of scan rate and (B) current vs. square root of scan rate.

$$\log\ k_s = \alpha\ \log(1-\alpha) + (1-\alpha)\log\ \alpha - \log(RT/n_\alpha F\nu) - \alpha(1-\alpha)n_\alpha F\Delta E_p/2.3RT \quad (1)$$

Using the above equations, $\alpha$ and $k_s$ value were determined for each sensor. As it can be seen in Table 1, after immobilization of pDNA, the $k_s$ value significantly decreases.

The chronoamperometric method was used to determine the diffusion coefficient ($D$). By the concentration gradient of $[Fe(CN)_6]^{3-/4-}$ ions between bulk and interface, it could be calculated via the Cottrell equation (Bard and Faulkner, 2001).

The electroactive surface area ($A_e$) for the modified electrodes and biosensors could be calculated on the basis of the linear slope of the anodic peak currents versus the square root of the potential sweep rates (Fig. 3B). $A_e$ for the types of the electrodes and biosensors was obtained by using the calculated diffusion coefficient and a known concentration of $[Fe(CN)_6]^{3-/4-}$ via the Randles–Sevick Eq. (2) (Bard and Faulkner, 2001):

$$A = S/\left(\left(2.69\times 10^5\right)n^{3/2}CD^{1/2}\right) \quad (2)$$

where $C$ is the molar concentration of $[Fe(CN)_6]^{3-/4-}$, $S$ is the slope obtained from the linear regression of $I_p$ versus $\nu^{1/2}$, $A$ is the electrode surface area, $n$ is the electron transfer number, and $D$ is the diffusion coefficient. Using a 5.0 mM solution of $[Fe(CN)_6]^{3-/4-}$ in PBS (0.1 M, pH 7.4, 0.9% NaCl) and the slope obtained from the linear regression of $I_p$ versus $\nu^{1/2}$, $A_e$ was calculated. The results are shown in Table 1. The surface area of the Au electrode immersed in the electrolyte solution was 0.0314 $cm^2$, indicating that the presence of CdS QDs led to an increase in the active surface of the electrode. The $A_e$ value for the CdS-QDs/Au electrode as compared to that of the MPA/Au electrode was improved. According to the method used for the synthesis of CdS-QDs, there were so many carboxylic groups on the CdS-QDs, as it is obvious in Scheme S1. Furthermore, the zero dimensional nanostructure of QDs provided a high surface-to-volume ratio. Increasing the number of particles on the electrode surface led to an enhancement of the chemisorbed pDNA quantity on the CdS-QDs/Au modified electrode, as observed in SEM studies (Section S4 and Fig. S2).

### 3.3. Differential pulse voltammetry (DPV)

Differential pulse voltammetry (DPV) was used to investigate the electrochemical response of the fabricated pDNA/CdS-QDs/Au biosensor for detection of ApoB-100 gene using methylene blue (MB) as a redox hybridization indicator. MB is used as an electrochemical marker that can be reduced on the electrode surface by two electrons to leucomethylene blue (Erdem et al., 2001). It binds specifically to the guanine (G) bases in DNA (Zhang et al., 2009). The pDNA/CdS-QDs/Au biosensor was incubated in a Tris – HCl buffer (pH 7.4) containing $2.0\times 10^{-5}$ M MB. To increase the sensitivity and selectivity of the DNA biosensor, experimental conditions including the effect of MB accumulation time, effect of DNA probe concentration and hybridization time were optimized (Section S5 and Fig. S4).

**Table 1**
Values of the kinetic parameters calculated for the modified electrodes.

| Name of the electrode | Electron transfer coefficient ($\alpha$) | Charge transfer rate constant ($k_s$; $s^{-1}$) | Diffusion coefficient ($D$; $cm^2\ s^{-1}$) | Electroactive surface area ($A_e$; $cm^2$) |
|---|---|---|---|---|
| MPA/Au | 0.5648 | 0.07236 | $1.24\times 10^{-7}$ | 0.092 |
| CdS-QDs/Au | 0.5786 | 0.12197 | $1.37\times 10^{-7}$ | 0.12 |
| pDNA/MPA/Au | 0.5801 | 0.00431 | $1.45\times 10^{-8}$ | 0.083 |
| pDNA/CdS-QDs/Au | 0.5897 | 0.010746 | $2.12\times 10^{-8}$ | 0.075 |

One of the main purposes of fabricating new biosensors is to recognize differences between target DNA and others. In order to study the specificity, hybridization tests were performed with perfect complementary target (pcDNA) and noncomplementary DNA (ncDNA) sequences. Fig. 4A presents a comparison of the differential pulse voltammograms of equal concentrations of each oligonucleotide. 1 μM was subjected to hybridization with the pDNA immobilized on the biosensor surface, and the corresponding signal of MB reduction current value was recorded. In the presence of ncDNA, the electrochemical signal of the pDNA/CdS-QDs/Au biosensor was found to decrease by about 3.14% while, in the presence of perfect matched target DNA (pcDNA), the signal decreased about 50.66%.

It should be noticed that the significant current difference obtained for pcDNA ($\Delta$ = 15.01 μA) is ascribed to the fact that the interaction between the MB molecules and the nucleoside residues of the probe was prevented by hybrid formation at the biosensor surface. This was actually due to the inaccessibility of the guanine bases in double-stranded DNA (dsDNA). Such behavior confirms that the constructed biosensor can be used to identify the target DNA with high specificity and good selectivity.

To evaluate the performance of the fabricated biosensor, the differential pulse voltametric response in the presence of MB, after hybridization with the target DNA, was measured at different concentrations. The quantitative results were documented by a

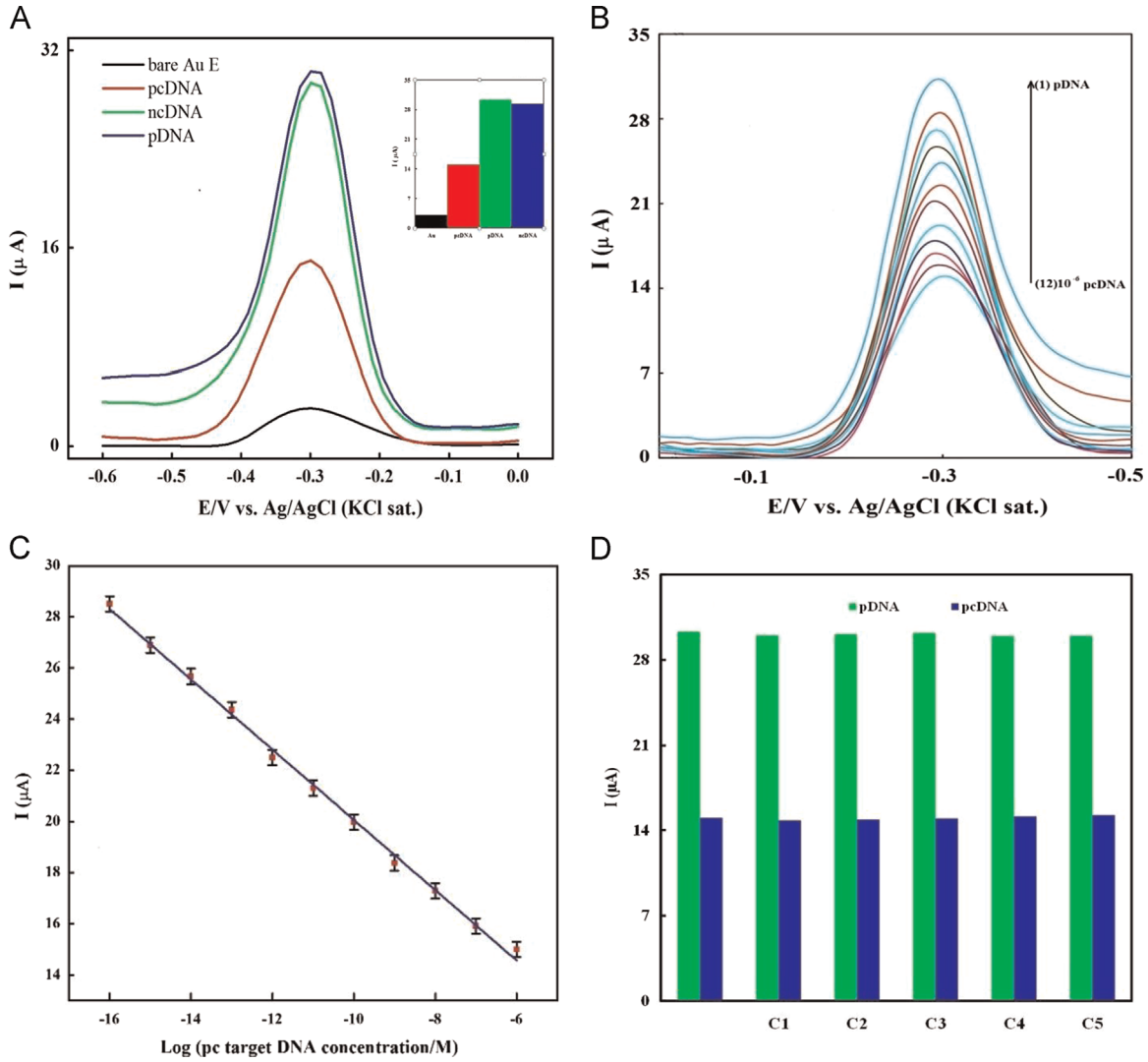


**Fig. 4.** (A) Differential pulse voltammograms for a bare Au sensor and a pDNA/Cd-SQDs/Au biosensor after incubation with 1 μM concentration of pcDNA and ncDNA. (B) Sensing characteristics of a pDNA/CdS-QDs/Au biosensor as a function of target DNA concentration in the range from $1.0 \times 10^{-16}$ to $1.0 \times 10^{-6}$ M. (C) The linearity plot for the variation in the MB peak height with respect to the log of the target DNA concentration. (D) Variation in the MB peak current of the pDNA/CdS-QDs/Au biosensor with repeated cycling for hybridization and regeneration.

calibration experiment over a concentration range of $10^{-16}$–$10^{-6}$ M target DNA.

Fig. 4B presents a decrease in the electrochemical signals with an increase in the complementary DNA concentrations. The resulting calibration plots (Fig. 4C) exhibit a good linear relationship between the peak current values (pertaining to the reduction of MB) and the target nucleotide concentrations in the range of $10^{-16}$–$10^{-6}$ M. The correlation coefficient ($R^2$) in this range was found to be 0.9973 using the following Eq. (4):

$$I_{\mathrm{pDNA/CdS/Au}}(\mu\mathrm{A}) = 6.3257(\mathrm{A}) - 1.3737(\mathrm{A})[\log(\text{pc target DNA concenteration})] \quad (4)$$

The control experiment was carried out by immobilizing pDNA onto the Au electrode using 3-mercaptopropionic acid as a cross-linker i.e. pDNA/MPA/Au. The experimental details are available in Section S6 and Fig. S4. The improved characteristics obtained for the pDNA/CdS-QDs/Au biosensor, as compared to those of the pDNA/MPA/Au biosensor, may be attributed to the high surface-to-volume ratio of CdS-QDs as well as accumulation of carboxylic acid groups around CdS-QDs which leads to creation of a more suitable space for complete immobilization of pDNA. Thus, increasing the effective surface area available for signal transduction and quantity improvement of chemisorbed pDNA ultimately lead to improved detection limits.

The obtained results using a pDNA/CdS-QDs/Au biosensor are comparable with the results reported in the literature (Sharma et al., 2013). The pDNA/CdTe/As/ITO biosensor showed a linear relationship with the concentrations of the target DNA in the range of $1.0 \times 10^{-12}$–$1.0 \times 10^{-6}$ M. While in this work, quantum dots directly attached to the gold electrode without any linkers, so electrode preparation was easier and the dynamic detection range of the sequence-specific DNA was from $1.0 \times 10^{-16}$ to $1.0 \times 10^{-6}$ M.

Owing to the strong chemisorption of pDNA on the CdS-QDs/Au electrode surface, this kind of electrode is stable enough to allow for ready regeneration. For this purpose, the electrode can be immersed in a buffer solution (50 mM Tris–HCl, pH 7.4) at 95 °C for five minutes, followed by cooling in the ice bath for about 10 minutes. This completely removes hybridized DNA via thermal denaturation (Sharma et al., 2012; Zoski, 2007). Fig. 4D demonstrates the variation in the MB peak current of the pDNA/CdS-QDs/Au biosensor for hybridation and denaturation processes. To investigate the reproducibility of the pDNA/CdS-QDs/Au biosensor,

the DPV signals of MB were recorded after five cycles of hybridization/dehybridization. The total loss of hybridization signal of hybridization/dehybridization was found to be about 0.7 μA, which corresponded to ~4.6% of the initial value. This is a proof that the biosensor reproducibly detects target DNA over repeated uses.

### 3.4. DNA synthesis of apolipoprotein B-100 with DNA polymerase and characterization by electrochemical impedance spectroscopy

Due to its uniform surface and uniform immobilization of the probe on its surface because of QDs presence, a pDNA/CdS-QDs/Au biosensor was applied to investigate DNA hybridization, monitoring of DNA synthesis and detection mutation of ApoB-100 based on the length increasing of the probe by the electrochemical impedance spectroscopy (EIS) method.

EIS is a useful technique providing exact information on the impedance changes of the sensor surface. In a typical impedance spectrum, a semicircle part at high frequencies and a straight line at low frequencies are related to the electron transfer-limit process and diffusion-limit process respectively. $R_{CT}$ can be estimated by the semicircle diameter of the impedance spectra at high frequencies. The $R_{CT}$-to-redox indicator is affected by surface blocking effects exerted by the hybridization of target DNA with the probe and the charged state of the probe layer on the electrode.

Two biosensors were fabricated in the optimal conditions with two amine-terminated probe DNAs (one for the normal sequence (npDNA) and one for the mutant sequence) and employed for the hybridization study of the corresponding sequences. EIS was employed to investigate the $R_{CT}$ of $[Fe(CN)_6]^{3-/4-}$ as a redox probe at the surface of these biosensors. Fig. 5 presents the Nyquist plots obtained for these biosensors in PBS (100 mM, pH 7.4, 0.9% NaCl) solution containing 5 m M $[Fe(CN)_6]^{3-/4-}$.

Fig. 5A illustrates the Nyquist plots obtained for the npDNA/CdS-QDs/Au biosensor from the hybridizations of 1 μM normal target DNA with the immobilized probe. As it can be seen, an increase in $R_{CT}$ value is observed after the attachment of CdS-QDs on the Au electrode. This may be attributed to the semiconducting nature of CdS-QDs, which leads to a slower electron transfer from the electrolyte to the electrode surface (curve b, $R_{CT}$=9.26 kΩ). When the planar CdS-QDs/Au electrode surface was immobilized by npDNA, the $R_{CT}$ value was increased compared to the CdS-QDs/Au electrode (curve c, $R_{CT}$=14.20 kΩ). It suggests the formation of an insulating layer of pDNA on the electrode surface, which leads to a decrease in electron transfer. Curve d shows the Nyquist plot of the npDNA/CdS-QDs/Au biosensor after hybridization with the 1 μM of designed synthetic normal target DNA (ntDNA) that generally leads to a sharp increase in the amount of $R_{CT}$ (22.46 kΩ). The ntDNA is a longer sequence than npDNA and has a part of complementary sequence that can be hybridized with npDNA. An increase in the amount of $R_{CT}$ indicates that the hybridization of ntDNA with the npDNA/CdS-QDs/Au biosensor was successfully completed and double-stranded DNA (dsDNA) was created. Compared to the dsDNA/CdS-QDs/Au biosensor, the $R_{CT}$

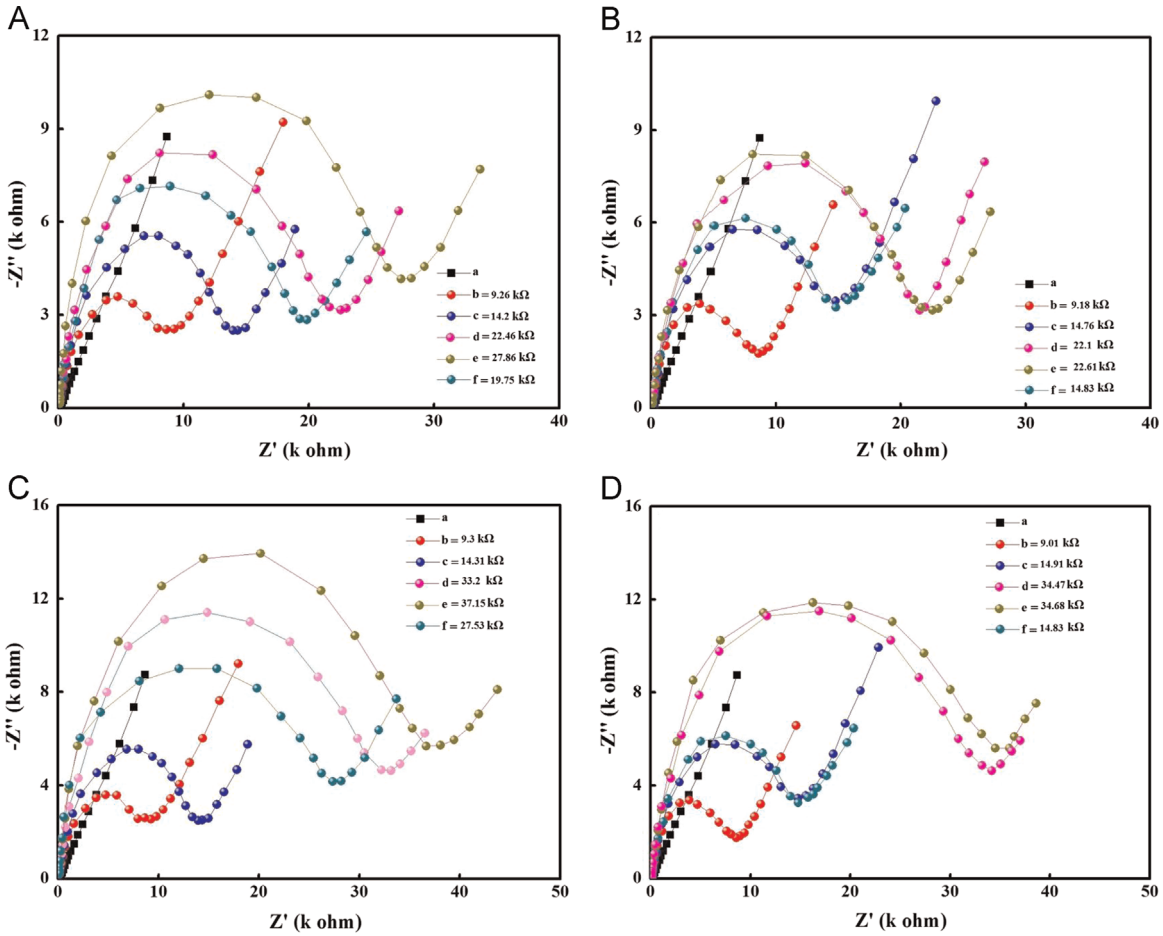


**Fig. 5.** Nyquist plots for normal designed synthetic sequences (A), mutant designed synthetic sequences (B), normal PCR products (C) mutant PCR products (D): (a) bare Au electrode, (b) CdS/Au electrode, (c) npDNA/CdS-QDs/Au biosensor, (d) dsDNA/CdS-QDs/Au biosensor, (e) after synthesis process and (f) after denaturation process in a PBS (100 mM, pH 7.4, 0.9% NaCl) solution containing 5 m M $[Fe(CN)6]^{3-/4-}$ at scanning frequencies from 0.01 to 100,000 Hz (the $R_{CT}$ values for each sensor are shown in the legends).

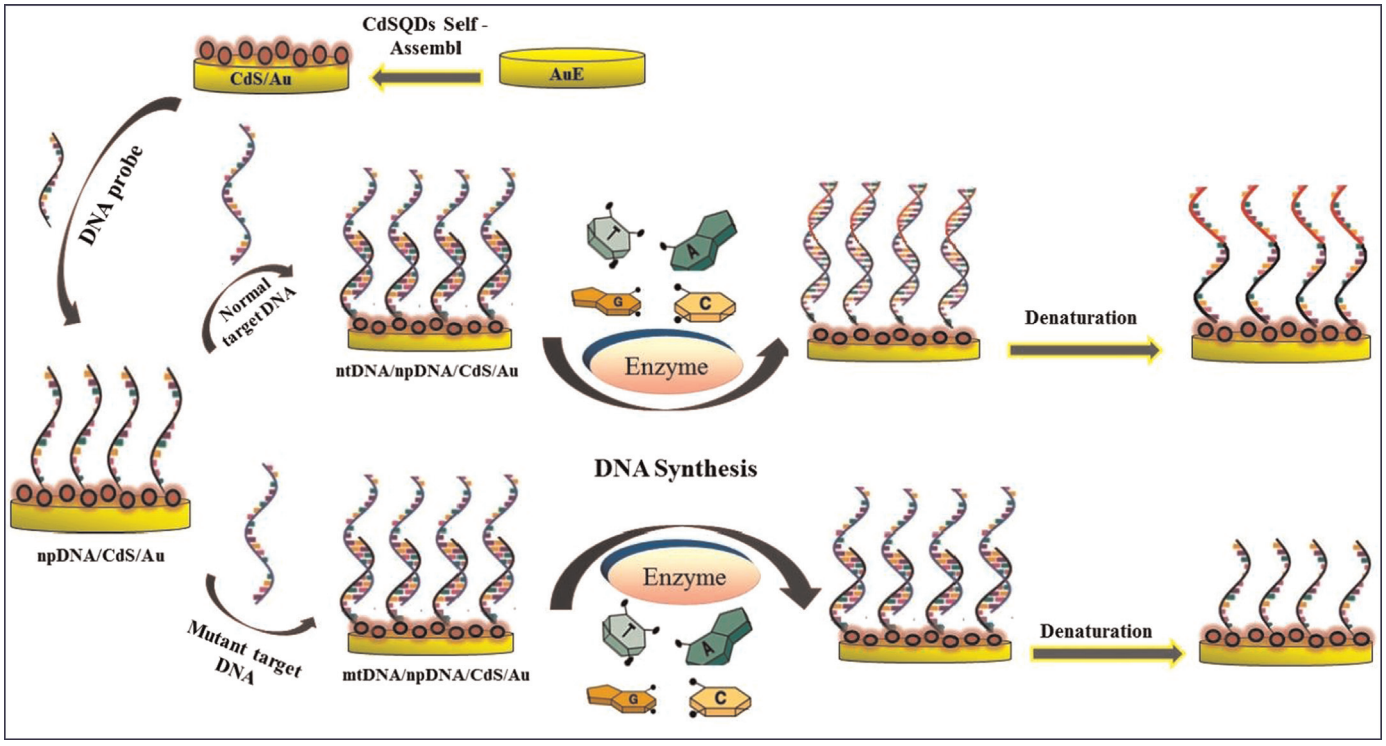


**Scheme 1.** Schematic diagram of DNA synthesis and denaturation on a pDNA/CdS-QDs/Au biosensor.

value of the biosensor increased after DNA synthesis by Klenow enzyme and deoxyribonucleotide triphosphate (dNTP) according to the model shown in Scheme 1 (curve e, $R_{CT}$= 27.86 kΩ). Afterwards, denaturation of dsDNA was performed by immersing the biosensor in water at 95 °C for five minutes. It led to denaturation of dsDNA and elimination of target DNA.Therefore, only the extended probes were maintained on the biosensor surface. As expected, the $R_{CT}$ value after the denaturation step (curve f, $R_{CT}$=19.75 kΩ) was larger than the $R_{CT}$ value for the npDNA/CdS-QDs/Au biosensor (curve c, $R_{CT}$=14.20 kΩ). This increase indicated that the extended DNA probe after synthesis was longer than the initial DNA probe (npDNA). Therefore, it confirms the synthesis of DNA by enzyme along the probe. Another biosensor (npDNA/CdS-QDs/Au) in the optimal conditions was fabricated, in a similar way for the designed synthetic mutant sequence (Scheme 1). The results are shown in Fig. 5B. The impedance spectra were recorded for this biosensor after probe immobilization (curve c, $R_{CT}$=14.76 kΩ) and hybridization (curve d, $R_{CT}$=22.10 kΩ) processes. These processes brought about the same results as obtained for the normal sequence. Afterwards, Klenow enzyme and dNTP were added on the surface of the dsDNA/CdS-QDs/Au biosensor for fabrication of strains complementary DNA. However, this process was not performed, and it suggests a mutation. The impedance spectra for the synthesis (curve e, $R_{CT}$=22.61 kΩ) and denaturation (curve f, $R_{CT}$=14.83 kΩ) processes were similar to the hybridation (curve d) and probe immobilization (curve c) processes respectively. These results suggest that mutant sequence cannot proceed DNA synthesis. Therefore, normal sequence and mutant sequence are distinguishable by this method. Prior to performing the electrochemical assay with PCR amplicons of ApoB-100 gene, DNA was separated from 200 μL of blood by a DNA extraction kit. Polymerase chain reaction (PCR) amplification of ApoB-100 gene was performed using a pair of primers. The PCR products hybridized with probe DNA were immobilized on the npDNA/CdS-QDs/Au biosensor and then analyzed by the EIS technique. As expected, the obtained results for normal PCR products (Fig. 5C) were similar to normal synthesized sequences (Fig. 5A) with the exception of higher $R_{CT}$ obtained for normal PCR products. Also, the obtained results for mutant PCR products (Fig. 5D) were similar to mutant synthesized sequences (Fig. 5B). The Nyquist plots (Fig. 5C and D) confirm the ability of the npDNA/CdS-QDs/Au biosensor to distinguish the normal PCR product sequence from the mutant PCR product sequence. All this proves that the present biosensing assay is suitable for the detection of R3500Q mutation of ApoB-100 Gene.

## 4. Conclusion

In the present study, we have developed an extremely sensitive electrochemical biosensor for detection of R3500Q mutation of ApoB-100 gene, DNA hybridization and investigation of DNA synthesis using a QDs self-assembly based electrochemical assay. The designed synthetic ApoB-100 specific probe was covalently immobilized on the CdS-QDs modified Au electrode and characterized by SEM, cyclic voltammetry and electrochemical impedance spectroscopy. CdS-QDs have some advantages such as a high surface-to-volume ratio, good biocompatibility and excellent ability for probe immobilization, which result in high-level sensitivity, stability and accuracy in determination of ApoB-100 gene. Under optimal conditions, the nucleic acid biosensor was specifically hybridized with target complementary DNA in a wide concentration range. Such QDs-based biosensors promise to make a reliable tool to be applied in clinical investigations.

## Acknowledgments

The authors would like to thank Yazd University Research Council, IUT Research Council and Excellence in Sensors for the financial support of this research.

## Appendix A. Supporting information

Supplementary data associated with this article can be found in the online version at 10.1016/j.bios.2015.05.014.

## References


Algar, W.R., Massey, M., Krull, U.J., 2009. Trends Anal. Chem. 28, 292–306.
Amouzadeh-Tabrizi, M., Shamsipur, M., 2015. Biosens. Bioelectron. 69, 100–105.
Asphahani, F., Thein, M., Veiseh, O., Edmondson, D., Kosai, R., Veiseh, M., Xu, J., Zhang, M., 2008. Biosens. Bioelectron. 23, 1307–1313.
Bard, A.J., Faulkner, L.R., 2001. Electrochemical Methods: Fundamentals and Applications, second ed. Wiley, New York.
Benvidi, A., Rajabzadeh, N., Mazloum-Ardakani, M., Heidari, M.M., Mulchandani, A., 2014. Biosens. Bioelectron. 58, 145–152.
Brus, L.E., 1984. J. Chem. Phys 80, 4403–4409.
Wang, P., Liu, Q., 2010. Cell-Based Biosensors Principles and Applications. Artech House, Boston.
Chan, W.C.W., Maxwell, D.J., Gao, X.H., Bailey, R.E., Han, M.Y., Nie, S.M., 2002. Curr. Opin. Biotechnol. 13, 40–46.
Chen, D., Wang, G., Li, J.H., 2007. J. Phys. Chem. C 111, 2351–2367.
De, M., Ghosh, P.S., Rotello, V.M., 2008. Adv. Mater. 20, 4225–4241.
Erdem, A., Kerman, K., Meric, B., Ozsoz, M., 2001. Electroanalysis 13, 219–223.
Fischer, M.J., 2010. Methods Mol. Biol. 627, 55–73.
Gerion, D., Parak, W.J., Williams, S.C., Zanchet, D., Micheel, C.M., Alivisatos, A.P., 2002. J. Am. Chem. Soc 124, 7070–7074.
Gill, R., Zayats, M., Willner, I., 2008. Angew. Chem. Int. Ed. 47, 7602–7625.
Horvath, A.D., Kirov, S.A., Karaulanov, E.E., Ganev, V.S., 2001. J. Clin. Lab. Anal. 15, 256–259.
Huang, H., Bai, W., Dong, C., Guo, R., Liu, Z., 2015. Biosens. Bioelectron. 68, 442–446.
Katz, E., Willner, I., Wang, J., 2004. Electroanalysis 16, 19–44.
Kim, J.H., Morikis, D., Ozkan, M., 2004. Sens. Actuators B—Chem. 102, 315–319.
Klostranec, J.M., Chan, W.C.W., 2006. Adv. Mater. 18, 1953–1964.
Kramer, I.J., Sargent, E.H., 2011. ACS Nano 5, 8506–8514.
Laviron, E., 1979. J. Electroanal. Chem. Interfacial Electrochem. 101, 19–28.
Li, G., Li, X., Wan, J., Zhang, Sh, 2009. Biosens. Bioelectron. 24, 3281–3287.
Lin, C.A.J., Lied, T., Sperling, R.A., Fernandez-Arguelles, M.T., Costa-Fernandez, J.M., Pereiro, R., Sanz-Medel, A., Chang, W.H., Parak, W.J., 2007. J. Mater. Chem. 17, 1343–1346.
Mazloum-Ardakani, M., Rajabzadeh, N., Benvidi, A., Heidari, M.M., 2013. Anal. Biochem. 443, 132–138.
Mazloum-Ardakani, M., Hosseinzadeh, L., Taleat, Z., 2014a. Microchim. Acta 181, 917–924.
Mazloum-Ardakani, M., Sheikh-Mohseni, M.A., Mirjalili, B.F., 2014b. Ionics 20, 431–437.
Mazloum-Ardakani, M., Aghaei, R., Abdollahi-Alibeik, M., Moaddeli, A., 2015. J. Electroanal. Chem. 738, 113–122.
Medintz, I.L., Uyeda, H.T., Goldman, E.R., Mattoussi, H., 2005. Nat. Mater. 4, 435–446.
Murrar, C.B., Norris, D.J., Bawendi, M.G., 1993. J. Am. Chem. Soc. 115, 8706–8715.
Myant, N.B., 1993. Atherosclerosis 104, 1–18.
Pathak, S., Choi, S.K., Arnheim, N., Thompson, M.E., 2001. J. Am. Chem. Soc. 123, 4103–4104.
Prasuhn, D.E., Feltz, A., Blanco-Canosa, J.B., Susumu, K., Stewart, M.H., Mei, B.C., Yakovlev, A.V., Loukou, C., Mallet, J.M., Oheim, M., Dawson, P.E., Medintz, I.L., 2010. ACS Nano 4, 5487–5497.
Schubert, K., Khalid, W., Yue, Z., Parak, W.J., Lisdat, F., 2010. Langmuir 26, 1395–1400.
Sharma, A., Pandey, C.M., Matharu, Z., Soni, U., Sapra, S., Sumana, G., Pandey, M.K., Chatterjee, T., Malhotra, B.D., 2012. Anal. Chem. 84, 3082–3089.
Sharma, A., Sumana, G., Sapra, S., Malhotra, B.D., 2013. Langmuir 29, 8753–8762.
Soria, L.F., Ludwig, E.H., Clarke, H.R., Vega, G.L., Grundy, S.M., Mcarthy., B.J., 1989. Proc. Natl. Acad. Sci. USA 86, 587–591.
Taleat, Z., Cristea, C., Marrazza, G., Mazloum-Ardakani, M., Săndulescu, R., 2014. J. Electroanal. Chem. 717-718, 119–124.
Thavanathan, J., Huang, N.M., Thong, K.L., 2014. Biosens. Bioelectron. 55, 91–98.
Tybjaerg-Hansen, A., Humphries, S.E., 1992. Atherosclerosis 96, 91–107.
Wang, Y., Herron, N., 1991. J. Phys. Chem. 95, 525–532.
Wang, F., Tan, W.B., Zhang, Y., Fan, X.P., Wang, M.Q., 2006. Nanotechnology 17, R1–R13.
Yu, W., Peng, X., 2002. Angew. Chem. Int. Ed. 41, 2368–2371.
Yu, W.W., Qu, L.H., Guo, W.Z., Peng, X.G., 2003. Chem. Mater. 15, 2854–2860.
Zhang, F., Ali, Z., Amin, F., Riedinger, A., Parak, W.J., 2010. Anal. Bioanal. Chem. 397, 935–942.
Zhang, L.F., Zuo, S.H., Yuan, H.H., Lan, M.B., Geoffrey, A., Lawrance, C., Wei, G., 2009. Bioelectrochemistry 74, 223–226.
Zhai, Y., Zhang, Y., Qin, F., Yao, X., 2015. Biosens. Bioelectron. 70, 130–136.
Zhong, X., Liu, S., Knoll, W., 2004. J. Mater. Chem. 14, 2790–2794.
Zoski, C.G., 2007. Handbook of Electrochemistry. Elsevier, Amsterdam/Boston.